JOURNAL OF GUIDANCE, CONTROL, AND DYNAMICS
Vol. 17, No. 1, January–February 1994

# Integrated Flight/Propulsion Control: Subsystem Specifications

Stephen M. Rock*
*Stanford University, Stanford, California 94305*
Abbas Emami-Naeini†
*Integrated Systems, Inc., Santa Clara, California 95054*
and
Ken Neighbors‡
*Stanford University, Stanford, California 94305*

**In many systems it is required or desirable to implement a control law in a partitioned or decentralized architecture comprised of subsystems. This paper presents a technique for deriving specifications for each subsystem that, if met, guarantee that total system performance (e.g., stability) goals will be met when the subsystems are combined. The approach is based on the concepts of robust control theory and generates results that are expressed in the frequency domain as allowed error envelopes about nominal requirements. Although emphasis is placed on generating specifications that guarantee only the stability of the combined system, extensions that would guarantee performance are also discussed. The focus of the paper is the integrated flight/propulsion control problem in which specifications on the propulsion system are derived based on the mission-level requirements of the aircraft. However, the results are generally applicable. A numerical example demonstrating the application of the procedure is included.**

## I. Background: The Need for Specifications

A CURRENT trend in aircraft system design is to integrate the functions of the flight and propulsion systems through their controls with the intent of improving the operational capabilities of the overall system. Such integration has been shown[1] to yield significant improvements in supermaneuverable air-to-air operation and in short takeoff and vertical land (STOVL) operation. The performance gains obtainable through this integration are results of recent technological advances that permit greater flexibility in the use of propulsion generated thrusts as primary flight control effectors. Examples include vectoring nozzles and various propulsive lift schemes such as ejectors, remote augmented lift systems (RALS), and various techniques of boundary-layer control using engine air.[2]

One obvious result of this integration is that the flight and propulsion systems become much more coupled than ever before. The propulsion system becomes an integral part of the flight control providing forces and moments about several axes rather than just providing axial thrust. Although many technological advances are required to enable this capability, one of the most critical is the development of a control design procedure that addresses the issues that result from this introduced coupling and provides a practical approach to control system design. The preliminary development of an integrated flight/propulsion control (IFPC) design procedure based on a decentralized approach is addressed in Refs. 3–5. Alternate techniques based on centralized approaches are addressed in Refs. 6–8.

Two issues make a decentralized approach to IFPC design attractive. The first is that flight and propulsion control design problems are very different. Flight control designs are typically regulators with input shaping where the design objective is to match flying and handling quality criteria that are often expressed in terms of equivalent system models.[10] Propulsion control is primarily nonlinear limit tracking.[11] Hence, writing a single performance index that completely defines the details of both problems is difficult.

The second issue that supports a decentralized approach is that the aircraft and the propulsion systems are built and supplied by different responsible manufacturers. Hence, design accountability issues dictate that each party retain control over all aspects of the system for which it is responsible. Specifically, each manufacturer will need to design and deliver the control logic that affects its plant.

For partitioning to be possible in an integrated control design, a mechanism must be introduced for communicating performance requirements and operational constraints among the designers that guarantees that overall performance goals will be met in the presence of the coupling and modeling uncertainty that exist. Presented here is a technique for generating such specifications. Also presented is an example that demonstrates an application of the technique to the propulsion control system design in an IFPC system.

Note that the derivation of the specifications that follows is based on linear system theory assumptions, whereas actual implementations can involve significant nonlinearities in the control system. In short, linear analysis tools are being used to evaluate the performance of a nonlinear system. Although potentially restrictive, this approach is justifiable and powerful. For example, under certain conditions, it is possible to deduce information about the stability of a nonlinear system from an associated linear model. Restrictions enter, however, in the need to specify the class of inputs used to evaluate the nonlinear system. As a simple example, the stability of a nonlinear system can be dependent on the input amplitude. Consequently, if frequency domain techniques are used, stability must be checked for "all" input amplitudes in addition to all frequencies. Direct nonlinear techniques might improve the results, but such procedures are not currently available.

## II. Problem Statement

A decentralized approach for implementing an IFPC logic is presented in Fig 1. This structure is consistent with that proposed in Ref. 5. It suggests a hierarchical approach in which a mission-level plant $P(s)$ is controlled using the outputs of a set

Received Oct. 24, 1990; revision received Feb. 25, 1993; accepted for publication Feb. 25, 1993. 

*Associate Professor, Department of Aeronautics and Astronautics. Senior Member AIAA.
†Research Scientist, Advanced Systems Group.
‡Ph.D. Candidate, Department of Aeronautics and Astronautics. Member AIAA.

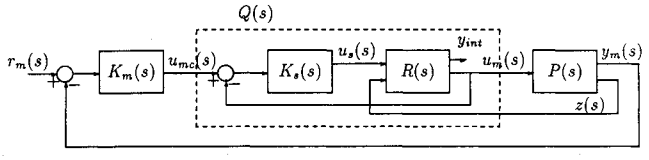


**Fig. 1 Hierarchical IFPC design.**

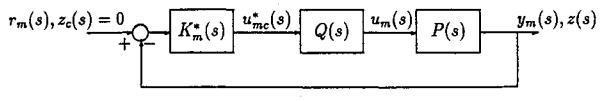


**Fig. 2 Mission-level design problem.**

of subsystems $R(s)$. In an IFPC system, the mission-level plant would be the aircraft, and the subsystems would consist of all of the aerodynamic surfaces plus the propulsion system. The mission related outputs $y_m$ would include variables that define aircraft handling qualities, flying qualities, tracking accuracy, etc. The subsystem outputs $y_s$ would include the forces and moments generated on the aircraft plus variables that define the performance of the aerodynamic surface control loops and the performance of the propulsion system.

There are two compensators indicated in the figure: $K_m(s)$ and $K_s(s)$. $K_m(s)$ is a mission-level compensator that addresses the control of outputs $y_m$ using the forces and moments $u_m$, which are created by the subsystems. That is, the mission-level controls $u_m$ are a subset of the subsystem outputs $y_s$

$$y_s = \begin{bmatrix} u_m \\ y_{\text{int}} \end{bmatrix} \tag{1}$$

where $y_{\text{int}}$ are the outputs internal to the subsystems and do not affect directly the mission-level performance (e.g., surge margins, pressures, temperatures, and speeds within the engine).

The second compensator $K_s(s)$ is a subsystem level compensator (or group of compensators for a decentralized system) that addresses simultaneously the control of the subsystem specific variables $y_{\text{int}}$ and the generation of the interface control variables $u_m$.

Let the mission-level plant be defined as

$$\begin{aligned} y_m(s) &= P_1(s)u_m(s) \\ z(s) &= P_2(s)u_m(s) \end{aligned} \tag{2}$$

and

$$P(s) \triangleq \begin{bmatrix} P_1(s) \\ P_2(s) \end{bmatrix} \tag{3}$$

Let the combined set of subsystems be defined as

$$\begin{aligned} u_m(s) &= R_{11}(s)u_s(s) + R_{12}(s)z(s) \\ y_{\text{int}}(s) &= R_{21}(s)u_s(s) + R_{22}(s)z(s) \end{aligned} \tag{4}$$

and

$$R(s) \triangleq \begin{bmatrix} R_{11}(s) & R_{12}(s) \\ R_{21}(s) & R_{22}(s) \end{bmatrix} \tag{5}$$

From Eq. (4) and the fact that $u_s(s) = K_s(s)[u_{mc}(s) - u_m(s)]$, the response of the closed-loop subsystems to a commanded $u_{mc}$ is found to be

$$\begin{aligned} u_m(s) = {} & [I + R_{11}(s)K_s(s)]^{-1}R_{11}(s)K_s(s)u_{mc}(s) \\ & + [I + R_{11}(s)K_s(s)]^{-1}R_{12}(s)z(s) \end{aligned} \tag{6}$$

In these equations, $z$ defines the vector of terms that couples the plant output into the subsystems. This coupling is described by $P_2(s)$, $R_{12}(s)$, and $R_{22}(s)$. For some applications, the plant and the subsystems can be assumed to be one-way coupled, and these terms set to zero. This assumption is reasonable when integrating the propulsion and flight controls in fixed-wing aircraft for some configurations, but it is not always true.[12] The assumption is valid when the forces and moments generated by the engine are not affected by the motion of the aircraft.

The advantage of the integrated control problem defined in Fig. 1 is that it permits the mission-level and the subsystem-level problems to be addressed separately. Consider first the mission-level problem. It is identified in Fig. 2. Note two things about this figure. First, the closed-loop subsystems have been replaced by a set of equivalent actuator characteristics $Q(s)$ that define the nominal performance assumed achievable by the subsystem control designers. Second, note that the coupling path $z(s)$ has been moved in this figure into the outer loop (its command is zero). This approach allows systems with two-way coupling to be addressed, and requires that

$$K_m^*(s) = \begin{bmatrix} K_m(s) & 0 \\ 0 & -I \end{bmatrix} \tag{7}$$

and

$$u_{mc}^* = \begin{bmatrix} u_{mc} \\ z \end{bmatrix} \tag{8}$$

The solution to this mission-level problem involves both the compensator $K_m(s)$ and the set of nominal equivalent closed-loop actuator characteristics $Q(s)$ that together satisfy the mission-level goals. The compensator $K_m(s)$ is defined as

$$u_{mc}(s) = K_m(s)[r_m(s) - y_m(s)] \tag{9}$$

and the nominal actuator characteristics are defined as

$$u_m(s) = Q_1(s)u_{mc}(s) + Q_2(s)z(s) \tag{10}$$

and

$$Q(s) \triangleq [Q_1(s)\ Q_2(s)] \tag{11}$$

where $Q_2(s)$ is usually the zero matrix and $Q_1(s)$ is typically diagonal. That is, the typical desired response of $u_m$ is that it tracks its commands $u_{mc}$ and rejects the coupling terms $z$ as disturbances. If the system is one-way coupled, $Q(s) = Q_1(s)$, $K_m^*(s) = K_m(s)$, and $u_{mc}^*(s) = u_{mc}(s)$.

Two techniques have been suggested for solving the mission-level design problem and generating $K_m(s)$ and $Q(s)$. Reference 10 treats $Q_1(s)$ as an assumed achievable performance [$Q_2(s) = 0$] of the subsystems and then designs a $K_m(s)$ that will meet the mission-level objectives using these assumed actuator characteristics. This approach requires an a priori knowledge of what will be reasonable performance to expect from the subsystems. An alternate approach is proposed in Ref. 9 in which the nominal closed-loop performance characteristics $Q_1(s)$ are derived along with the $K_m(s)$ as part of a centralized design approach. In either case, a $Q(s)$ is created that becomes the nominal closed-loop requirement that the subsystem designer is expected to match. If this nominal performance is not achievable by the subsystem designers, then iteration on the mission-level design will be required. (This could include the relaxation of the mission-level performance goals.)

Consider second the subsystem control design problem. From Eqs. (6) and (10), it can be expressed as finding a compensator $K_s(s)$ that meets a tracking requirement

$$[I + R_{11}(s)K_s(s)]^{-1}R_{11}(s)K_s(s) \approx Q_1(s) \tag{12}$$

and a disturbance rejection requirement

$$[I + R_{11}(s)K_s(s)]^{-1}R_{12}(s) \approx Q_2(s) \tag{13}$$

The tracking requirement defines how well each subsystem must produce those elements in $u_m$ for which it is responsible. The disturbance rejection requirement defines how well each subsystem must isolate itself from the other subsystems and from the mission-level plant. In an integrated control problem the disturbances of interest include not only external sources but also the effects of the coupling among the various subsystems. That is, if the problem is decentralized, then a specification is required that defines how strongly one subsystem is allowed to excite another, or conversely, how much one subsystem is allowed to respond to activity in another.

The issue addressed in the following is determining the accuracy with which Eqs. (12) and (13) must be satisfied. These tolerances, when combined with the nominal requirements, represent a set of specifications for the subsystem designer to meet that will guarantee the performance (e.g., stability) of the integrated system. These are specifications that must be met in addition to all of the normal subsystem specific specifications that a subsystem designer addresses (e.g., protecting surge margins, etc.).

## III. Subsystem Specifications

An equivalent representation of allowing uncertainty when matching $Q(s)$ is through an additive uncertainty matrix $\Delta Q_T(s)$, which acts in parallel with the generalized actuators $Q(s)$ (see Fig. 3). Any transfer function matrix $T(s)$ relating $u_m(s)$ to $u^*_{mc}(s)$ can be written in the form $T(s) = Q(s) + \Delta Q_T(s)$ or $\Delta Q_T(s) = T(s) - Q(s)$.

A bound on $\|\Delta Q_T(s)\| = \bar{\sigma}\{\Delta Q_T(s)\}$ can be found that will guarantee integrated system stability by noting that $\Delta Q_T(s)$ is identical in form to the additive uncertainty models used in robust control analyses. Therefore, if the specifications are derived in a fashion consistent with robustness analysis, they will be sufficient for defining the small-amplitude characteristics of the integrated system.

The issue is how to calculate the bound on $\|\Delta Q_T(s)\|$ and then how to distribute this bound into individual scalar bounds for each transfer function of $T(s)$.

The proposed procedure is based on the concept of inverting the procedures of robust control system design. In standard robust control design, a control law is found that can accommodate a specified level of uncertainty. Here, a bound on the uncertainty that can be tolerated in the generalized actuators by an existing control design is computed.

### A. Calculation of an Additive Uncertainty $\Delta Q_T(s)$

Consider the closed-loop system defined in Fig. 3. The mission-level plant $P(s)$ is described by Eqs. (2) and (3); the nominal equivalent actuator characteristics $Q(s)$ are described by Eqs. (10) and (11); and the mission-level compensator $K^*_m(s)$ is defined by Eqs. (7) and (9). Given this, a matrix $\Delta Q_B$ of bounds on the additive uncertainty on the equivalent actuator characteristic $\Delta Q_T(s)$ can be found through a stability robustness analysis.

The first step is to calculate a scalar upper bound on the norm of the matrix $\Delta Q_T(s)$ for $s = j\omega$ that will preserve stability of the closed-loop system. Defining $\ell(\omega)$ to be this bound and applying the procedures of Ref. 13 to additive uncertainty yields (see Ref. 14)

$$\ell(\omega) = \frac{1}{\bar{\sigma}\{K^*_m(j\omega)P(j\omega)[I + Q(j\omega)K^*_m(j\omega)P(j\omega)]^{-1}\}} \tag{14}$$

where $\bar{\sigma}$ is the maximum singular value of the matrix.

Given $\ell(\omega)$, any stable matrix $\Delta Q_T(s)$ that satisfies $\|\Delta Q_T(j\omega)\| < \ell(\omega)$ will result in a stable closed-loop system.

To write individual scalar bounds for the elements of $T(s)$, a desired distribution of tolerances must first be specified. Let

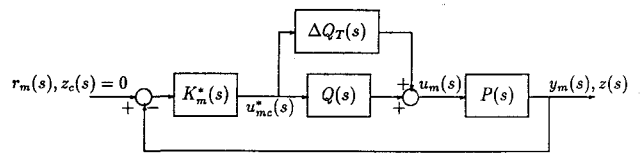


**Fig. 3 Additive uncertainty on $Q(s)$.**

the matrix $\overline{\Delta Q}$ define this distribution. For example, a choice of $\overline{\Delta Q} = [I\ 0]$ would allow equal errors in tracking all commanded controls $u_{mc}$ but would require that all coupling effects be rejected exactly [zeros are desired on the off-diagonals of $Q_1(s)$ and in all of $Q_2(s)$]. A choice of $\overline{\Delta Q}$ having $\overline{\Delta Q}(i,j) = 1$ for all $i$ and $j$ would allow equal errors in tracking and disturbance rejection. [Since $\overline{\Delta Q}$ may have structure, the structured singular value $\mu$ could be used in place of $\bar{\sigma}$ in Eq. (14) and evaluated with respect to the structure to reduce conservativeness. This is illustrated in the example in Sec. IV.)

Since $\overline{\Delta Q}$ specifies the relative magnitudes of the error tolerances, each element of $\overline{\Delta Q}$ must be nonnegative. Also, to simplify numerical issues, all system matrices should be normalized to remove units.

Given $\overline{\Delta Q}$, next define $\Delta Q_B(\omega) = \ell(\omega)\overline{\Delta Q}/\|\overline{\Delta Q}\|$. This definition allows the tolerances defined in $\overline{\Delta Q}$ to remain fixed relative to each other, but to vary with frequency. Now, $\|\Delta Q_B(\omega)\| = \ell(\omega)$, and any matrix $\Delta Q_T(j\omega)$, with $\|\Delta Q_T(j\omega)\| < \|\Delta Q_B(\omega)\|$, will guarantee stability.

One way to ensure that $\|\Delta Q_T(j\omega)\| < \|\Delta Q_B(\omega)\|$ is for the magnitude of each element of $\Delta Q_T$ to be less than the corresponding element of $\Delta Q_B$, i.e., $|\Delta Q_{Tij}(j\omega)| < \Delta Q_{Bij}(\omega)$. This element-by-element requirement allows scalar bounds to be written in the desired form. The actual transfer function matrix $T(s) = Q(s) + \Delta Q_T(s)$ will have the form illustrated by this $2 \times 2$ example:

$$Q + \Delta Q_T = \begin{bmatrix} Q_{11} + \Delta Q_{T11} & Q_{12} + \Delta Q_{T12} \\ Q_{21} + \Delta Q_{T21} & Q_{22} + \Delta Q_{T22} \end{bmatrix} \tag{15}$$

To get the tracking specification, the bound on the additive uncertainty must be mapped into upper and lower bounds on magnitude and phase. For a given nominal, scalar transfer function $Q_{ij}(s)$, where $Q_{ij}(s) \neq 0$, the value of the actual transfer function $T_{ij}(s)$ can be expressed as

$$\begin{aligned} T_{ij}(s) &= Q_{ij}(s) + \Delta Q_{Tij}(s) \\ &= \left[1 + \frac{\Delta Q_{Tij}(s)}{Q_{ij}(s)}\right] Q_{ij}(s) \end{aligned} \tag{16}$$

Since $Q_B$ bounds $Q_T$, this equation can also be written for $s = j\omega$ as

$$T_{ij}(j\omega) = f(\omega) \times Q_{ij}(j\omega) \tag{17}$$

where $f(\omega)$ is any complex number of the form $1 + r(\omega)$ that satisfies $|r(\omega)| < R(\omega)$ with

$$R(\omega) \triangleq \frac{\Delta Q_{Bij}(\omega)}{|Q_{ij}(j\omega)|} \tag{18}$$

That is, if $f(\omega)$ is represented as a vector drawn from the origin it must terminate within a circle of radius $R(\omega)$ about 1. This is shown in Fig. 4. Case 1 in the figure corresponds to $R(\omega) < 1$, and case 2 corresponds to $R(\omega) \geq 1$.

For both cases, magnitude and phase bounds define a sector region inside this circle. If $R(\omega) < 1$, the maximum allowed phase deviation occurs if the magnitude boundary is tangent to the circle. That is

$$\phi_{\max}(\omega) = \sin^{-1}R(\omega)$$

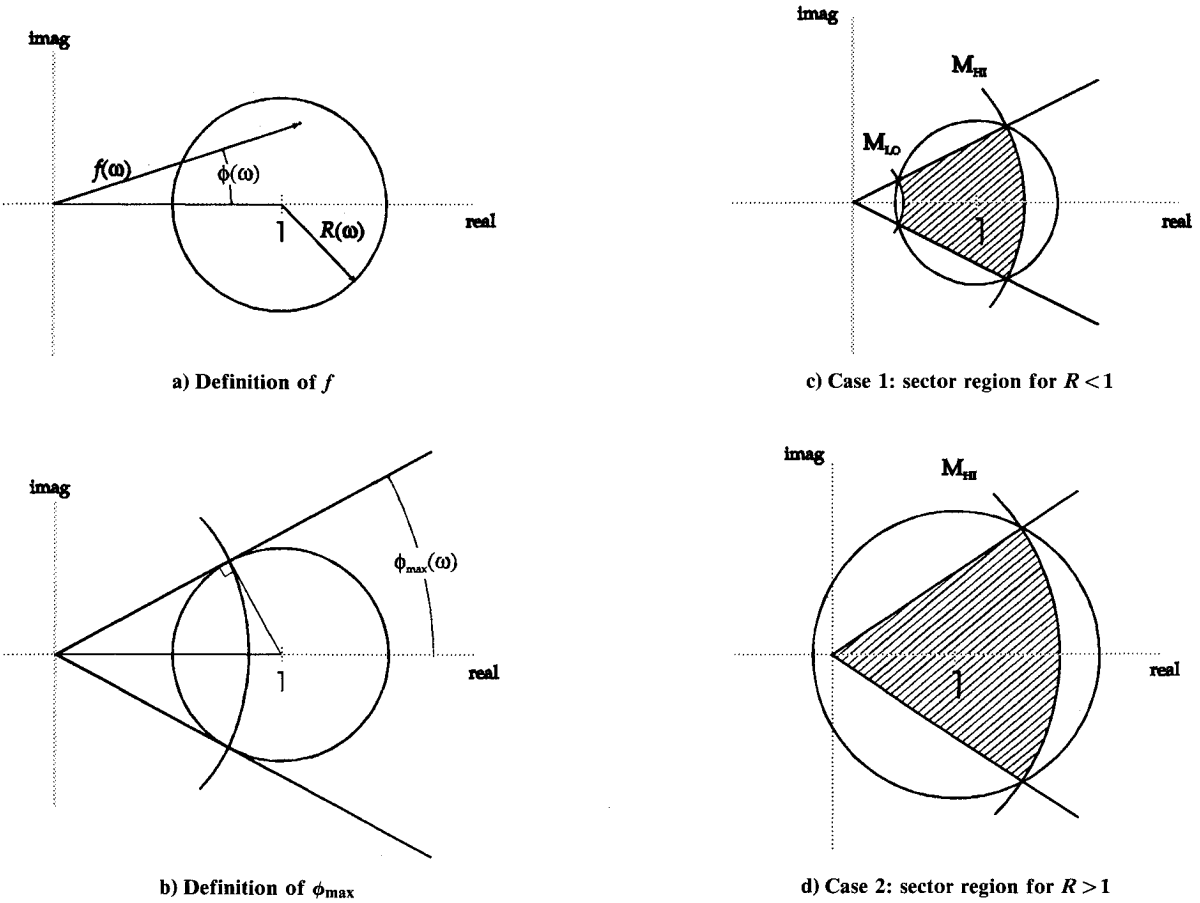


**Fig. 4 Use of sector regions to calculate magnitude and phase bounds.**

with a magnitude of

$$M(\omega) = \sqrt{1 - R^2(\omega)}$$

For a given phase bound $\phi(\omega) < \phi_{\max}(\omega)$ the upper and lower magnitude bounds $M_{HI}(\omega)$ and $M_{LO}(\omega)$ are found using the relation

$$R^2(\omega) = M^2(\omega) + 1 - 2M(\omega)\cos\phi(\omega) \tag{19}$$

$M_{HI}(\omega)$ and $M_{LO}(\omega)$ are just the maximum and minimum solutions of Eq. (19). Note that Eq. (19) is similar to a result in Ref. 15 that was derived within the framework of multiloop stability margins.

If $R(\omega) \geq 1$ the upper magnitude bound is the positive solution of Eq. (19), and the lower magnitude bound is zero.

From Fig. 4, it is evident that the magnitude and phase bounds are conservative since the sector does not completely cover the circle. It is also evident that, using sector regions, the bounds are not unique. If the magnitude bounds are relaxed, it is necessary to tighten the phase bounds. One approach to minimizing the conservativeness and establishing uniqueness is to select magnitude and phase bounds that maximize the area of the sector region. Alternatively, this tradeoff can be used to give the subsystem control designer more freedom to meet the specifications.

If $Q_{ij}(j\omega) = 0$, bounds on the magnitude and phase are derived in a similar fashion. For this case, $|T_{ij}(j\omega)| < \Delta Q_{Bij}(\omega)$. The phase is arbitrary ($-180$ deg $\leq \phi \leq 180$ deg).

Once the bounds for each $T_{ij}(j\omega)$ have been found, they may be displayed as a frequency response plot with upper and lower limits on both magnitude and phase.

Note that the conservativeness associated with using the sector regions can be eliminated if $R(\omega)$ is issued as the specification. The difficulty with this approach is that it is no longer possible to represent simply the specification using classical techniques such as the frequency response Bode plot.

### B. Alternate Uncertainty Forms

The previous discussion has assumed that the allowable error in achieving the nominal subsystem characteristics $Q(s)$ is expressed as an additive uncertainty $\Delta Q_T(s)$ (see Fig. 3). Other forms, such as input-multiplicative and output-multiplicative uncertainties on $Q(s)$, are also possible.

These forms are similar in that each describes an error in achieving the nominal $Q(s)$. There are differences in detail, however. For example, multiplicative uncertainty describes a percentage error in achieving the nominal, whereas additive uncertainty describes an absolute error. The best choice is case dependent.

The steps to calculate bounds corresponding to multiplicative uncertainty are similar to those for the additive uncertainty treated earlier. The equivalent transfer function matrix of the subsystems for input-multiplicative uncertainty is

$$T(s) = Q(s)[I + L_{T_I}(s)] \tag{20}$$

and for output-multiplicative uncertainty is

$$T(s) = [I + L_{T_O}(s)]Q(s) \tag{21}$$

In either case a matrix $\overline{\Delta L}$ must first be specified that defines the desired distribution of tolerances (it replaces $\overline{\Delta Q}$). Then a matrix $\Delta L_B$ of bounds on the multiplicative uncertainty can be found as

$$\Delta L_B(\omega) = \frac{\ell(\omega)\overline{\Delta L}}{\|\overline{\Delta L}\|} \tag{22}$$

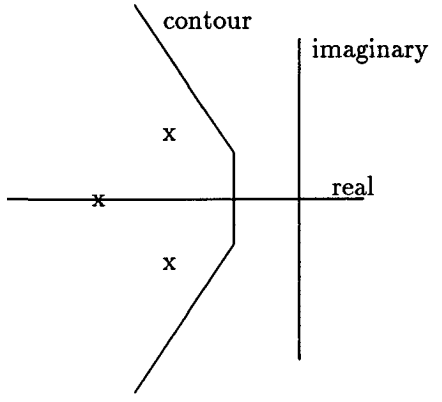


**Fig. 5 Performance region defined in the $s$ plane.**

For input-multiplicative uncertainty on $Q(s)$

$$\ell_I(\omega) = \frac{1}{\bar{\sigma}\{K_m^*(j\omega)P(j\omega)Q(j\omega)[I + K_m^*(j\omega)P(j\omega)Q(j\omega)]^{-1}\}} \tag{23}$$

For output-multiplicative uncertainty on $Q(s)$

$$\ell_o(\omega) = \frac{1}{\bar{\sigma}\{Q(j\omega)K_m^*(j\omega)P(j\omega)[I + Q(j\omega)K_m^*(j\omega)P(j\omega)]^{-1}\}} \tag{24}$$

Any $T(j\omega)$ [Eq. (20) or (21) depending on the form chosen] that satisfies $\|L_T(j\omega)\| < \|L_B(\omega)\|$ guarantees stability.

### C. Performance vs Stability Robustness

The previous analysis generates bounds that guarantee stability of the mission-level design only. Extending this analysis to guarantee performance is possible for a variety of performance measures. The major issue is determining the measures of performance appropriate for a given problem. Several choices are possible.[17]

Two types of performance measures are described briefly here to demonstrate how the extensions might be accomplished. The detailed development and demonstration of these approaches is currently under development.

The first performance measure to consider is a requirement that all closed-loop system poles lie to the left of a specified contour in the $s$ plane, as shown in Fig. 5. Such a region could be defined to guarantee a minimum damping ratio and settling time on all of the system modes.

Calculating the scalar upper bound $\ell(s)$ on the norm of the matrix $\Delta Q_T(s)$ for this case requires simply that the gain of the nominal closed-loop transfer function be calculated along the specified contour rather than along the $j\omega$ axis. The inverse of this gain is the bound for the uncertainty, which will guarantee that the poles lie to the left of the contour. This is a well-known result of the small gain theorem. Specifically, Eq. (14) must be modified so that the specified contour replaces $j\omega$ in the calculation

$$\ell(s) = \left.\frac{1}{\bar{\sigma}\{K_m^*(s)P(s)[I + Q(s)K_m^*(s)P(s)]^{-1}\}}\right|_{s=\text{contour}} \tag{25}$$

The remainder of the procedure to generate the specifications remains the same except that all quantities must be calculated along the new contour in the $s$ plane instead of along the $j\omega$ axis.

The second performance measure to consider is a model-matching requirement that places a bound on the system's desired closed-loop transfer function matrix $H(s)$ from the command $r(s)$ to the outputs $y(s)$. For example

$$\|H(j\omega) - I\| < |W_P(j\omega)|^{-1} \tag{26}$$

where $W_P$ defines a limit on model tracking error.

The procedure to design a controller that meets this robustness requirement is described in Ref. 16. A fictitious uncertainty $\Delta_P(s)$ satisfying $\|\Delta_P(j\omega)\| \leq 1$ is introduced that converts the system shown in Fig. 3 into that shown in Fig. 6. Using structured singular value $\mu$-analysis, an $\ell(\omega)$ bound on $\|\Delta Q_T(j\omega)\|$ can be found that replaces Eq. (14). Given this $\ell(\omega)$, the rest of the procedure is unchanged. Note that a general result is that the bounds that guarantee performance lie inside the bounds that guarantee stability. That is, performance bounds are generally more restrictive than stability bounds.

## IV. Example

Consider the IFPC system described in Fig. 7. It is a longitudinal aircraft model that has three aerodynamic surfaces plus a propulsion system capable of producing two thrusts. The surfaces are the horizontal tail ($\delta H$), the leading edge flaps ($\delta N$), and the trailing edge flaps ($\delta F$). Thrust $F_1$ is axial and acts through the center of gravity. Thrust $F_2$ is normal and acts approximately 10 ft behind the center of gravity. Models for this example were generated at an altitude of 100 ft, a Mach number of 0.18, and a flight path angle of 3 deg. The mass was assumed to be 839 slugs.

In this example, the propulsion system is treated as a subsystem that generates thrusts $F_1$ and $F_2$ in response to commands. Each aerodynamic control surface is also treated as a subsystem. The mission-level design problem is to control the aircraft attitude. Each subsystem-level control problem is to respond to commands for the effector quantities (e.g., $F_1$ and $F_2$ for the propulsion subsystem) in addition to providing internal control of that subsystem.

The objective of this example is to demonstrate how specifications can be generated that define how well the propulsion system must generate $F_1$ and $F_2$ in response to commands and how well each aerodynamic surface must respond to its command. Note that detailed models of the subsystems are not involved in the example. They are only required when performing the detailed control design of each subsystem.

The equations of motion describing this system were defined in Eq. (2). (This system is one-way coupled.) An equivalent state variable representation is

$$\dot{x}_m = A_p x_m + B_p u_m$$

$$y_m = C_p x_m + D_p u_m = [I]x_m + [0]u_m$$

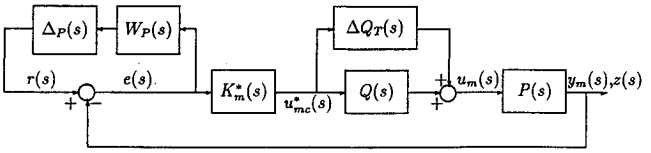


**Fig. 6 Introduction of a fictitious uncertainty to include performance robustness.**

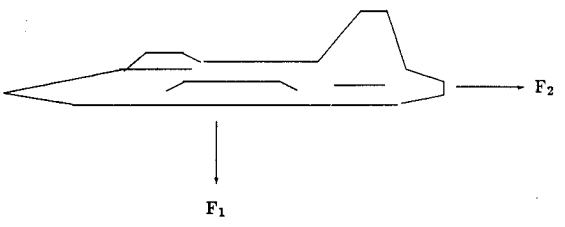


**Fig. 7 Aircraft with axial and vertical thrust.**

**Table 1 Open- and closed-loop eigenvalues**

| Open loop | Closed loop |
|---|---|
| −1.4720 | −0.2047 + 0.1993*i* |
| 1.0652 | −0.2047 − 0.1993*i* |
| −0.0568 + 0.2154*i* | −2.3352 |
| −0.0568 − 0.2154*i* | −4.3661 + 1.4738*i* |
| −15.0000 | −4.3661 − 1.4738*i* |
| −15.0000 | −9.8604 |
| −15.0000 | −14.1960 |
| −10.0000 | −14.9876 |
| −10.0000 | −14.9994 |

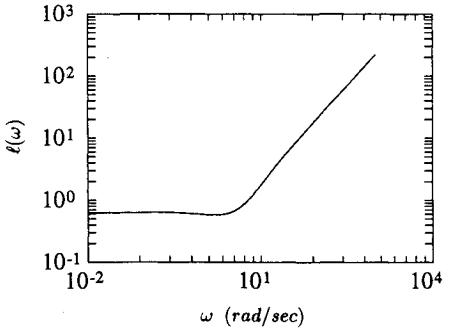


**Fig. 8 Scalar stability bound for the IFPC example.**

where

$$x_m = \begin{bmatrix} u \\ w \\ q \\ \theta \end{bmatrix} = \begin{bmatrix} \text{forward velocity, ft/s} \\ \text{vertical velocity, ft/s} \\ \text{pitch rate, rad/s} \\ \text{pitch angle, rad} \end{bmatrix}$$

$$u_m = \begin{bmatrix} \delta H \\ \delta N \\ \delta F \\ F_1/m \\ F_2/m \end{bmatrix} = \begin{bmatrix} \text{horizontal tail, deg} \\ \text{leading edge flaps, deg} \\ \text{trailing edge flaps, deg} \\ \text{axial acceleration, ft/s}^2 \\ \text{normal acceleration, ft/s}^2 \end{bmatrix}$$

$$y_m = x_m$$

and

$$A_p = \begin{bmatrix} -0.0589 & 0.1068 & -38.5980 & -31.8390 \\ -0.2659 & -0.2665 & 194.8100 & -4.5989 \\ -0.0015 & 0.0078 & -0.1949 & -0.0005 \\ 0.0000 & 0.0000 & 1.0000 & 0.0000 \end{bmatrix}$$

$$B_p = \begin{bmatrix} 0.1136 & 0.0347 & -0.0496 & 1.0000 & 0.0000 \\ -0.2321 & 0.0693 & -0.1455 & 0.0000 & -1.0000 \\ -0.0229 & -0.0081 & 0.0007 & 0.0000 & -0.0720 \\ 0.0000 & 0.0000 & 0.0000 & 0.0000 & 0.0000 \end{bmatrix}$$

The first step in the procedure is to complete a mission-level design that provides both a compensator $K_m(s)$ and a set of nominal equivalent actuator characteristics $Q(s)$ (see Fig. 1). Since the mission-level design is not the focus of this example, a very simple linear quadratic regulator (LQR) design was performed. This design yielded a state feedback control law of the form

$$u_{mc} = -K_m(s)y_m = -K_x x$$

since $y_m = x$. Here

$$K_x = \begin{bmatrix} 0.1594 & -0.1826 & -43.4240 & -27.1540 \\ 0.0596 & -0.0231 & -14.5420 & -14.5370 \\ -0.0366 & -0.0383 & 0.7457 & 5.9117 \\ 0.1378 & 0.0101 & -1.1616 & -0.5160 \\ 0.0735 & -0.1659 & -34.1329 & -19.0037 \end{bmatrix}$$

(Note that a practical compensator would most likely feed back such quantities as load factor, airspeed, and various integral states rather than the state variables as done here.) The set of equivalent actuator characteristics defined in Eq. (10) was chosen to be (state variable matrix form)

$$A_Q = \text{diag}\ \{-15, -15, -15, -10, -10\}$$
$$B_Q = \text{diag}\ \{15, 15, 15, 10, 10\}$$
$$C_Q = \text{diag}\ \{1, 1, 1, 1, 1\}$$
$$D_Q = \text{diag}\ \{0, 0, 0, 0, 0\}$$

That is, each aerodynamic surface is assumed to have a nominal bandwidth of 15 rad/s, and the propulsion system is assumed to have a nominal bandwidth of 10 rad/s.

The open- and closed-loop eigenvalues for this mission-level system design are shown in Table 1.

The second step in the procedure is to calculate the bound $\ell(\omega)$. It is computed as defined in Eq. (14). The result is displayed in Fig. 8.

The third step in the procedure is to select a distribution of uncertainty as defined by $\overline{\Delta Q}$. For this example the distribution of uncertainty is chosen to be

$$\overline{\Delta Q} = \begin{bmatrix} 2 & 0 & 0 & 0 & 0 \\ 0 & 2 & 0 & 0 & 0 \\ 0 & 0 & 2 & 0 & 0 \\ 0 & 0 & 0 & 1 & 1 \\ 0 & 0 & 0 & 1 & 1 \end{bmatrix}$$

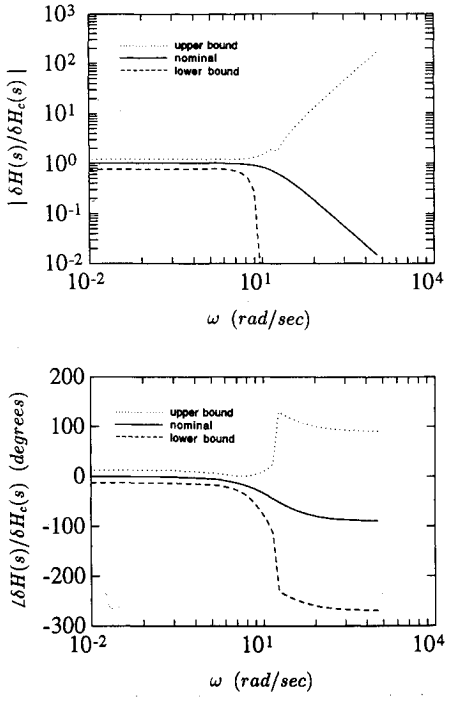


**Fig. 9 Aerodynamic surface tracking specification.**

(Note that the diagonal elements of the upper 3 × 3 block are set to 2 rather than 1. This reflects the desire to maximize the size of each entry in $\overline{\Delta Q}$, and hence the allowable error in the corresponding subsystem, without increasing its norm. The norm of this matrix is 2 for any $|\overline{\Delta Q}_{ii}| \leq 2$ for $i = 1, 2, 3$.)

This distribution matrix was chosen to take advantage of the fact that there is known to be no coupling between the aerodynamic surfaces and the propulsion system. The matrix indicates that each of the aerodynamic surfaces (the first three controls) will have a tolerance band on how well it must track its command, and that the response of each surface must be uncoupled. The distribution matrix also indicates that the accuracy with which the propulsion system must track its two thrust commands (the last two controls) is equal to the accuracy with which it must decouple the two thrust responses.

Finally, upper and lower bounds are calculated as described in Eqs. (16–18). The results are shown graphically in Figs. 9–11. The specification on the tracking performance of the aerodynamic actuators is presented in Fig. 9. The specification on the tracking performance of the engine ($F_1/F_{1c}$ and $F_2/F_{2c}$) is presented in Fig. 10. The specification on how well $F_1$ and $F_2$ must be decoupled is presented in Fig. 11. (Note that the lower bound is zero and that a linear scale has been used.)

These specifications indicate that at low frequencies (for example) the aerodynamic surfaces must track their commands within a range of 45–136% of nominal gain and ± 25 deg of phase. The propulsion thrusts must track their commands within a range of 75–120% of nominal gain and ± 12 deg of phase. Also, the $F_2$ thrust response to an $F_1$ thrust command must be less than 31% (and vice versa). These specifications were determined by maximizing the sector area (see Fig. 4).

Note that these specifications calculated earlier are known to be conservative. This results from two sources. First, expressing the specifications as magnitude and phase limits required using sectors (see Fig. 4). Second, the distribution matrix $\overline{\Delta Q}$ has structure.

The conservativeness caused by the structure in $\overline{\Delta Q}$ can be reduced by replacing $\bar{\sigma}$ with the structured singular value $\mu$ in Eq. (14), and then calculating $\mu$ with respect to the known structure. This calculation was done, and the resulting $\ell(\omega)$ was at most a factor of 1.25 lower than the $\ell(\omega)$ shown in Fig. 8.

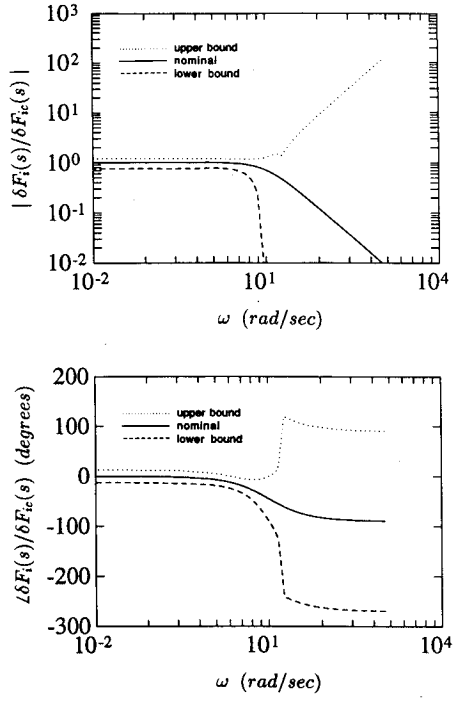


**Fig. 10 Thrust tracking specification.**

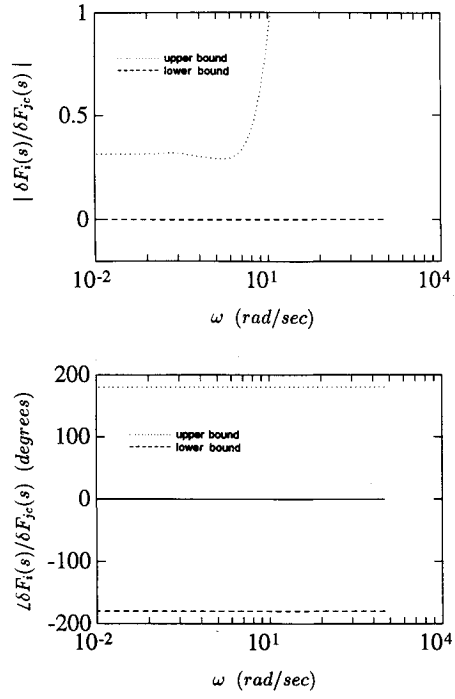


**Fig. 11 Thrust decoupling specification.**

Note that this result is very case dependent, however. The consequence of using this bound would be a slight broadening of the tolerance bounds (frequency dependent) shown in Figs. 9–11.

## V. Conclusions

A procedure based on the concepts of robust control theory has been developed that allows the generation of control design specifications for individual subsystems within the context of an integrated system design problem. In particular, subsystem specifications are generated that, if met, will guarantee stability when the subsystems are combined to form the integrated system. Extensions that would also guarantee performance were also discussed.

The form of the specifications generated is an allowed tolerance band about a nominal response characteristic and is expressed in the frequency domain. Specifications are generated for both tracking and disturbance rejection.

The numerical example demonstrated the application of this procedure to an IFPC problem. It involved the longitudinal control of an aircraft using three aerodynamic surfaces and two engine generated thrusts. Requirements on how well the aerodynamic surfaces must track their commands and on how well the propulsion system must track and decouple the thrust commands were generated.

## Acknowledgments

This research was supported in part by NASA Lewis Research Center under Grant NAG3-1177. The program monitors were Peter Ouzts and Michelle Bright. The models used in the example were supplied by Northrop Aircraft Division and were generated in the Air Force sponsored Design Methods for Integrated Control Systems program.[5]

## References

[1]Joshi, D. S., et al., "Design Methods for Integrated Control Systems, Part I: System Requirements and Simulation Development," Air Force Wright Aeronautical Lab., AFWAL-TR-84-2037, Wright-Patterson AFB, OH, Feb. 1985.

[2]Berg, D. F., Elliott, D. W., and Simmons, J. R., "Comparison Study of Supersonic STOVL Propulsion Systems," AIAA 24th Joint Propulsion Conf., AIAA Paper 88-2808, Boston, MA, July 1988.

[3]Rock, S. M., Emami-Naeini, A., and Anex, R. P., "Propulsion

Control Specifications in Integrated Flight/Propulsion Control Systems," AIAA 24th Joint Propulsion Conf., AIAA Paper 88-3236, Boston, MA, July 1988.

[4]Emami-Naeini, A., Anex, R. P., and Rock, S. M., "Integrated Control: A Decentralized Approach," *Proceedings of the 24th IEEE Conference on Decision and Control,* Dec. 1985, pp. 1836–1841.

[5]Shaw, P. D., et al., "Design Methods for Integrated Control Systems," Air Force Wright Aeronautical Lab., AFWAL-TR-88-2061, Wright-Patterson AFB, OH, June 1988.

[6]Smith, K. L., "Design Methods for Integrated Control Systems," Air Force Wright Aeronautical Lab., AFWAL-TR-86-2103, Wright-Patterson AFB, OH, Dec. 1986.

[7]Garg, S., Ouzts, P., Lorenzo, C., and Mattern, D., "IMPAC—An Integrated Methodology for Propulsion and Airframe Control," *Proceedings of the American Control Conference* (Boston, MA), June 1991.

[8]Garg, S., Mattern, D., Bright, M., Ouzts, P., "$H_\infty$ Based Integrated Flight/Propulsion Control Design for a STOVL Aircraft in Transition Flight," AIAA Guidance, Navigation, and Control Conf., AIAA Paper 90-3335, Portland, OR, Aug. 1990.

[9]Mattern, D., and Garg, S., "Propulsion System Performance Resulting from an Integrated Flight/Propulsion Control Design," *Proceedings of the AIAA Guidance, Navigation, and Control Conference* (Hilton Head, SC), AIAA, Washington, DC, 1992 (AIAA Paper 92-4602).

[10]Vincent, J. H., "Direct Incorporation of Flying Qualities Criteria Into Multivariable Flight Control Design," AIAA Guidance and Control Conf., AIAA Paper 84-1830, Aug. 1984.

[11]Rock, S. M., "Integrated Flight/Propulsion Control: Requirements and Issues," *Proceedings of XIth IFAC Symposium on Automatic Control in Aerospace* (Tsukuba, Japan), July 1989.

[12]Schmidt, D. K., and Schierman, J. D., "A Framework for the Analysis of Airframe/Engine Interactions and Integrated Flight/Propulsion Control," *Proceedings of the American Control Conference* (Boston, MA), June 1991.

[13]Doyle, J. C., and Stein, G., "Multivariable Feedback Design: Concepts for a Classical/Modern Synthesis," *IEEE Transactions on Automatic Control,* Vol. AC-26, No. 1, Feb. 1981, pp. 4–16.

[14]Morari, M., and Zafiriou, E ., *Robust Process Control,* Prentice-Hall, Englewood Cliffs, NJ, 1989, p. 244 (Fig. 11.1–4).

[15]Yeh, H. H., Ridgely, D. B., and Banda, S. S., "Nonconservative Evaluation of Uniform Stability Margins of Multivariable Feedback Systems," *Journal of Guidance, Control and Dynamics,* Vol. 8, No. 2, 1985, pp. 167–174.

[16]Doyle, J. C., Wall, J. E., and Stein, G., "Performance and Robustness Analysis for Structured Uncertainty," *Proceedings of the 21st IEEE Conference on Decision and Control,* 1982, pp. 629–636.

[17]Franklin, G. F., Powell, J. D., and Emami-Naeini, A., *Feedback Control of Dynamic Systems,* 2nd ed., Addison-Wesley, Reading, MA, 1991, Chap. 7.